Published in final edited form as:
Hum Mol Genet. 2005 November 1; 14(21): 3179–3189.

Dilated cardiomyopathy (DCM) in the *nmd* mouse: Transgenic rescue and QTLs that improve cardiac function and survival.

Terry P. Maddatu[1], **Sean M. Garvey**[2], **David G. Schroeder**[1], **Wiedong Zhang**[1], **Soh-Yule Kim**[3], **Anthony I. Nicholson**[1], **Crystal J. Davis**[1], and **Gregory A. Cox**[1,*]

1 *The Jackson Laboratory, 600 Main Street, Bar Harbor, ME 04609, USA*

2 *University Program in Genetics and Genomics, Duke University, Durham, NC 27710, USA*

3 *New York State Institute for Basic Research in Developmental Disabilities, Staten Island, NY 10314, USA.*

Abstract

Mutations in the immunoglobulin mu binding protein 2 (*Ighmbp2*) gene cause motor neuron disease and dilated cardiomyopathy (DCM) in the neuromuscular degeneration (*nmd*) mouse, and spinal muscular atrophy with respiratory distress (SMARD1) in humans. To investigate the role of IGHMBP2 in the pathogenesis of DCM, we generated transgenic mice expressing the full-length *Ighmbp2* cDNA specifically in myocytes under the control of the mouse *titin* promoter. This tissue-specific transgene increased the lifespan of *nmd* mice up to 8 fold by preventing primary DCM and showed complete functional correction as measured by ECG, echocardiography and plasma CK-MB. Double-transgenic *nmd* mice expressing *Ighmbp2* both in myocytes and neurons display correction of both DCM and motor neuron disease resulting in an essentially wild-type appearance. Additionally, quantitative trait locus (QTL) analysis was undertaken to identify genetic modifier loci responsible for preservation of cardiac function and a marked delay in the onset of cardiomyopathy in a CAST/EiJ backcross population. Three major CAST-derived cardiac modifiers of *nmd* were identified on Chromosomes 9,10 ,and 16, that account for over 26% of the genetic variance and that continue to suppress the exacerbation of cardiomyopathy, otherwise resulting in early death, as incipient B6.CAST congenics. Overall our results verify the tissue-specific requirement for IGHMBP2 in cardiomyocyte maintenance and survival, and describe genetic modifiers that can alter the course of DCM through cardiac functional adaptation and physical remodeling in response to changes in load and respiratory demand.

INTRODUCTION

Cardiomyopathies are morphologically and hemodynamically classified as DCM (the most common form in humans) and hypertrophic and/or restrictive (1). Regardless of apparent etiology, however, the ultimate sequela is congestive heart failure (CHF) and premature death. The mutation in the mouse *Ighmbp2* gene was cloned over seven years ago, followed by several reports of mutations and polymorphisms in its human counterpart, but so far its exact biological function is unknown (2–4). We recently reported the tissue-specific rescue of neuromuscular degeneration in *nmd* mice harboring a full-length *Ighmbp2* cDNA driven by the rat neuron-specific enolase (*Eno2*) promoter, C57BL/6J-Tg(*Eno2-Ighmbp2*), hereafter referred to as TgNI-*nmd* (5). This successful rescue of neurogenic atrophy in *nmd* mice established for the first time its cell autonomous nature in motor neuron survival. Likewise, we also described the

*To whom correspondence should be addressed. Fax: (207) 288-6073. E-mail:gac@jax.org..

CONFLICT OF INTEREST STATEMENT
The authors have no conflicts of interest to declare.

mapping of a major wild-type CAST-derived modifier locus on mouse Chromosome 13 (*Mnm*) that specifically halted motor neuron degeneration (2,5). Despite these genetic interventions however, the course and progression of DCM and CHF remained. Long-established mechanisms leading to cardiomyopathy include impaired force generation from defective sarcomeres (6), aberrant intracellular signaling and/or nuclear membrane disorders (7,8), mitochondrionopathy and deficits in cardiac energetics (9,10), facilitated cell death by apoptosis or necrosis (11), and/or inappropriate cellular response to growth, maturation and differentiation (12,13). Immunoglobulin mu binding protein-2 (IGHMBP2) is novel in that it is a predominantly cytoplasmic member of the DEXDc DEAD-like super family of DNA/RNA helicases possibly involved in RNA transport or translation and also implicated in the regulation of transcription and mRNA splicing (2,14). Therefore, mutant *nmd* mice, which express ~20% of normal IGHMBP2 levels due to a splice donor mutation (2), provide a valuable tool for gaining insight into the mechanisms of neuromuscular degeneration and dilated cardiomyopathy (DCM) (5). The onset, progression, and outcome of cardiomyopathy in humans is highly variable and subject to diverse modifications either intrinsic (genetic) or extrinsic (environmental) or both (15). Elucidating the etiology of these factors and their roles in the pathogenesis of DCM and CHF is pivotal to the successful clinical management of this complex disease (16). In a backcross with the wild-derived CAST/EiJ inbred strain, we observed a large variation in the maximum lifespan of *nmd* mice with altered onsets and severity of DCM. A genome-wide scan of affected N2 **c**ardiac **m**odified ***n****md* (*Cmn*) mice using lifespan as the quantitative trait identified three major QTLs (CAST-derived cardiac modifiers) on mouse Chromosomes 9, 10 and 16 that significantly delayed the onset of DCM and heart failure. Two similar studies looking at genetic modifiers affecting survival and cardiac function in a transgenic model of cardiomyopathy reported significant linkage on chromosomes 2 and 3 (17), and 4 and 18 to survival (18) as well as QTLs on chromosomes 2, 13, and 18 linked to "fractional shortening" and left ventricular end diastolic dimension (LVEDD) (18). Although both studies mapped QTLs on chromosome 2, none of these loci were identified in our study, highlighting the complexity and multigenic nature of cardiovascular remodeling in *nmd* mice. In addressing the cell-autonomous role of *Ighmbp2* in the pathogenesis of DCM, we show here that *nmd* mice expressing a full-length *Ighmbp2* cDNA under the control of the **m**uscle-specific mouse titin promoter C57BL/6J-**Tg**(*Ttn*-***I****ghmbp2*), hereafter referred to as TgMI, are rescued from fatal DCM. Furthermore, despite the presence of progressive neuromuscular degeneration, TgMI-*nmd* mice lived significantly extended life-spans, confirming the indispensable role of *Ighmbp2* in the survival of cardiomyocytes.

RESULTS

Muscle-Specific Rescue of Dilated Cardiomyopathy in nmd Mice.

As the *Ighmbp2* gene is ubiquitously expressed and motor neuron degeneration in *nmd* mice was rescued by expressing a full-length *Ighmbp2* cDNA transgene (TgNI) in neurons (5), we reasoned that myocytes might similarly have a tissue-specific requirement for IGHMBP. To address the role of *Ighmbp2* expression in cardiac and skeletal myocytes, we generated transgenic *nmd* mice expressing the full-length *Ighmbp2* cDNA under the control of the mouse titin (*Ttn*) promoter (TgMI). A schematic representation of the transgenic construct is shown in Figure 1A. RT–PCR analysis revealed that TgMI-derived *Ighmbp2* mRNA expression was limited to the heart and skeletal muscles in two independent transgenic lines (Fig. 1B, data not shown). To assess whether expression of the *Ighmbp2* transgene could rescue cardiomyocyte degeneration, B6-TgMI from lines 45 and 108 were independently crossed with heterozygous B6.BKS-*+/Ighmbp2*$^{nmd\text{-}2J}$ (hereafter referred to as B6-*+/nmd*) mice to produce TgMI-*nmd* mutant mice. Physical examination and longitudinal evaluation of overall health were compared between TgMI-*nmd*, double transgenic TgMI+NI-*nmd* and their sib-controls. In Figure 1C, the absence of neuron-specific expression of the *Ighmbp2* cDNA in both non-

transgenic *nmd* and TgMI-*nmd* mice led to severe skeletal muscle neurogenic atrophy-precluding the analysis of the potential role of skeletal myocytes in the progression of cardiomyopathy and consequent survival. In contrast, double transgenic TgMI+NI-*nmd* mice are indistinguishable from age-matched controls reflecting the combinatorial effects of the transgenes in preventing motor neuron disease and cardiomyopathy. The growth rate for TgMI-*nmd* mice, as measured by mean bodyweight, is comparable to that of non-transgenic *nmd* mice from 2 weeks of age onward, and is nearly half the mean bodyweight of the double transgenic *nmd* mice or their sib-controls (Figure 1D). Thus, the loss of spinal motor neurons and the resulting skeletal muscle atrophy seen in mutant *nmd* mice accounts for the reduced bodyweight in TgMI-*nmd* mice (5). Additionally, both male and female transgenic TgMI-*nmd* mice from lines 45 and 108 displayed equivalent growth rates, average life-spans (data not shown) and performance scores in functional tests; therefore mice from these two independent lines were combined for all subsequent analyses. Double transgenic *nmd* mice carrying both neuron and muscle-specific transgenes (TgMI+NI-nmd) displayed growth rates indistinguishable from their control littermates' (+/+ or +/*nmd*) at all time points (Figure 1D).

Transgenic Rescue of DCM: Morphological and Functional Assessments.

Longitudinal investigation of cardiac rescue in TgMI-*nmd* mice was initially assessed using maximum lifespan (Figure 2A). Compared to non-transgenic *nmd*, the cumulative survival curve of TgMI-*nmd* mice is significantly greater, but also significantly less than that of double transgenic TgMI+NI-*nmd* mice or their sib-controls (*nmd* vs TgMI-*nmd*, $p< 0.0001$, $Chi^2= 77.9$; TgMI-*nmd* vs TgMI+NI-*nmd*, $p < 0.0001$, $Chi^2= 28.7$; TgMI-*nmd* vs control, $p < 0.0002$, $Chi^2= 14.4$). To investigate the nature of these differences, routine necropsy and evaluation of not only the heart, but also other organs were conducted. Mean ventricular free-wall thickness in TgMI-*nmd* or TgMI+NI-*nmd* mice were not significantly different from *+/+ or +/nmd* transgenic sib-controls and were significantly thicker than those of B6-*nmd* hearts (Figure 2B, $p < 0.0001$). Although the mean weight of *nmd* hearts with the neuron-specific transgene were significantly less than that of double transgenic *nmd* (*p = .0126), they were not statistically different from those of TgMI-*nmd* or transgenic (+/+ or +/*nmd*) sib-control hearts (Figure 2C). Unexpectedly, the mean weights of double transgenic *nmd* hearts were greater than that of TgMI-*nmd* (**p = 0.0031) or that of control (**p = 0.0002). In fact, the mean weight of double transgenic *nmd* hearts was nearly 50% heavier (Figure 2C). In Figure 2D, this apparent increase in double transgenic *nmd* average heart-weight is proportionally distributed throughout all four chambers; such that individually, each weighed significantly more than that of TgMI-*nmd* or their sib-control (*p < 0.05-0.0005). This effect is unlikely to be due to an adverse effect of transgenic TgMI expression in the heart since the effect was not seen in singly-transgenic TgMI-*nmd* or TgMI-+/+ mice (Figure 2C) or in double-transgenic +/+ littermates (not shown). Therefore, this may reflect an unmet tissue-specific need for IGHMBP2 in other vital tissues/organs (i.e. liver, kidney, or adrenals) of *nmd* mice, indirectly altering heart size; or alternatively, this may reflect a compensatory increase in heart size due to the greater cardiac load and demand in the rescued double transgenic *nmd* mice, relative to paralyzed and activity restricted TgMI-*nmd* mice.

Morphological evaluations of TgMI-*nmd* hearts (fixed in tetany) indicated normal macroscopic presentation with ventricular chambers devoid of blood, the papillary muscles are large and prominent and the atria are comparably small (Figure 3A–C). These observations are consistent with the absence of histopathologic changes in ventricular myocytes stained with H&E (Figure 3D–F), cardiac functional integrity illustrated by normal conduction patterns in electrocardiograms (ECG, Figures 3G–H), and normal echocardiographic parameters (LVEDD, LVESD, Figures 3I–J). Nevertheless, TgMI-*nmd* mice were still vulnerable to late-onset complications from progressive neuromuscular degeneration including anorexia/dysphagia (difficulty in mastication or deglutition) culminating in wasting and malnutrition.

An apparent susceptibility to mega-esophagus as well as mastication and deglutition difficulties is completely eliminated in the presence of both neuron and muscle-specific transgenes with the concomitant rescue of neuromuscular degeneration and muscular dystrophy phenotypes (5). Hence, double transgenic TgNI+MI-*nmd* mice essentially lived greater than two years. Even with apparently enlarged hearts they fail to develop cardiomyopathy. However, an increased incidence of dermatitis possibly due to a B6 background effect, often necessitated their premature culling.

QTL Analysis Identifies Genetic Modifiers of Cardiomyopathy.

Disease penetrance and variation in phenotypic manifestations are commonly attributed to genetic background polymorphisms (15). We have previously shown that the *nmd* motor neuron disease can be suppressed by a CAST-derived modifier (Mnm^C) on Chr. 13 (2). To determine if the *nmd* cardiomyopathy is also amenable to genetic modification, we examined the maximum lifespan of 166 *nmd* mice from a segregating N2 backcross population (B6.CAST-Mnm^C/Mnm^C $Ighmbp2^{nmd\text{-}2J}$/+ x CAST/EiJ)F1 x (B6.CAST-Mnm^C/Mnm^C $Ighmbp2^{nmd\text{-}2J}$/+). N2 mutant *nmd* mice showed a wide range of life-spans ranging from as short as 2-weeks to as long as 57-weeks of age (Figure 4A), with most mutants ultimately developing cardiomyopathy. However, variation in the clinical manifestations of CHF strongly suggested the presence of CAST-derived genetic modifiers of DCM. Using survival as a biological indicator of cardiac improvement, quantitative trait locus (QTL) analysis of short-lived versus long-lived N2 mutant mice was performed. As shown in Figure 4B, following a genome-wide screen, long-lived *nmd* mice revealed similar segregation patterns for putative **c**ardiac **m**odifier of ***nmd*** (*Cmn)* QTLs on Chromosomes 9 (*Cmn1*) and 10 (*Cmn2*) and a QTL on Chromosome 16 (*Cmn3*) with a significant gender-effect (Figure 4C and Table 1). Confidence intervals (95%) of these three significant QTLs are shown in Figure 4D, plus two suggestive B6-derived QTLs on chromosomes 1 and 5 are shown in Figure 4E. *Cmn2* corresponds to a broad interval on Chr 10, potentially representing more than one QTL. We are currently constructing congenic lines harboring the CAST-derived QTLs on the neuron-specific modifier B6.CAST-Mnm^C background. Once full N10 congenic strains are established for these QTLs, their potential effects on DCM as well as the onset and progression of motor neuron disease can be assessed individually. The cumulative survival rates of cardiac modified *nmd* mice in the N2 and N3 segregating background generations are significantly greater than that of Mnm^C-*nmd* mice as shown in Figure 5A ($p < 0.0001$). Likewise, cardiac modified *nmd* mice carrying at least one CAST allele for each of the first three *Cmn* loci showed significantly greater mean life-spans than those of Mnm^C-*nmd* mice (228.2 ± 37.5 days vs. 68.6 ± 1.8 days, *$p < 0.0001$, Figure 5B). Overall these results suggest that, even at the N4 generation, wherein the genome is expected to be over 90% B6-like, the CAST-derived QTLs on Chrs. 9, 10 and 16, individually or in-combination, are still able to modify the onset and severity of DCM.

Morphological and functional assessment of DCM modification.

To investigate the nature of the cardiac improvement in N4F1 generation of *Cmn-nmd* mice, plasma CK-MB (brain/heart creatine kinase) levels were examined. As shown in Figure 6A, *nmd* mice between 4–8 weeks of age carrying the neuron-specific transgene TgNI showed the greatest average plasma CK-MB compared to non-transgenic *nmd* as shown previously (5). Although cardiac modified *nmd* mice had appreciably higher average plasma CK-MB levels compared to controls (367 ± 66.7 vs. 174.4 ± 10.6, ***$p = 0.0086$), they were significantly lower than TgNI-*nmd* (826.6 ± 380, *$p = 0.0002$) or *nmd* mice without the modifiers (620.8 ± 63.5, **$p = 0.0013$), suggesting that relatively fewer cardiomyocytes were undergoing degeneration. Since the neuron-specific TgNI construct rescues *nmd* paralysis, the observed increase in activity and cardiac demand hastens DCM, resulting in marked elevation in plasma CK-MB. With relatively fewer cardiomyocytes being lost, the cardiac morphology as well as

the ventricular free-wall thickness in the hearts of N3 to N5 generation *Cmn-nmd* mice were significantly rescued (*p < 0.0001) compared to *nmd* mice without the modifier loci (Figure 6B). The mean ventricular free-wall thickness and total heart weights of *Cmn-nmd* mice are not significantly different from control and reflect compensatory cardiac adaptation and remodeling (Figure 6C). This difference is further illustrated by increased left ventricular (LV) weight in *Cmn-nmd* versus B6-*nmd* hearts (*p = 0.0024). In contrast, both *Cmn-nmd* and B6-*nmd* mice showed significantly heavier mean atrial weights compared to normal sib-control (*p = 0.028) suggesting that the CAST-derived modifiers have no effect on atrial changes. Alternatively, subtle residual valvular insufficiency in *Cmn-nmd* hearts may promote compensatory atrial hypertrophy, which is more pronounced in B6-*nmd* mice (5). The mean right ventricular free-wall weights, and interventricular septum weights *of Cmn-nmd* hearts, as in B6-*nmd* hearts, are markedly reduced compared to sib-control hearts (**p < 0.014, Figure 6D). Assessment of cardiac function using ECG corroborated the observed atrial changes of either TgNI or *Cmn-nmd* mice with significantly greater P-wave amplitudes compared to control (*p < 0.002, **p < 0.009, Figure 6E). Both B6-*nmd* and *Cmn-nmd* showed greater mean left-ventricular volumes at diastole than control mice, consequently resulting in greater cardiac output (Figure 6F).

Gross and microscopic evaluation of the *Cmn-nmd* hearts revealed a wide range of morphological alterations but showed marked reduction in chamber dilation and nearly normal cardiac wall thickness (Figure 7A & 7C). However, most of these *Cmn-nmd* mice eventually develop CHF due to other causes, such as obstructive cardiomyopathy (due to organizing thrombi, Figure 7C, black arrow), restrictive cardiomyopathy (due to compensatory cardiomyocyte hypertrophy, Figure 7G), ischemic cardiomyopathy (due to myocardial infarction, Figure 6C, red arrows), or deficits in cardiac conduction (Figure 7I) resulting in sudden death. Closer examination of *Cmn-nmd* hearts revealed that putative cardiac modifiers may reduce the occurrence of replacement fibrosis as shown in Figure 7B versus 7E. Furthermore, functional evaluation of heart rates, blood pressure, electrocardiograms, as well as echocardiograms in these mice indicated normal systolic function, fully compensated hearts and remarkably normal cardio-respiratory function, in contrast to B6-*nmd* mice (Figure 7H-O, and data not shown). The diverse morphological changes in the hearts of long-lived *Cmn-nmd* reflect the effects of segregating CAST-derived cardiac modifiers. In the extremes, the *Cmn-nmd* heart in 7F appear morphologically normal, but functionally the strength of its conduction proved weak (7J) compared to the *Cmn-nmd* ECG in 7K or the normal B6 ECG in 7H. The echocardiogram (M-mode) in 7N depicts cardiac functional integrity in the presence of a mild, but noticeably increase in LVEDD and LVESD compared to *Cmn-nmd* heart in 7O or B6 control in 7L. Likewise, histopathology of long-lived *Cmn-nmd* ventricles in Figure 7G revealed the presence of hypertrophic cardiomyocytes which is consistent with that observed grossly in 7C. With impressive cardiac remodeling, still the amplitude of cardiac conduction in Figure 7K is only half that of the B6 control in 7L. The functional consequences of these changes are not clearly apparent in the normal echocardiogram in Figure 7O compared to 7L.

Early clinical signs of disease in *nmd* mice with or without cardiac modification included sudden death, respiratory distress, anorexia/dysphagia resulting in weight loss, anasarca (generalized subcutaneous edema) and cessation of normal activities. Given the wide range of maximum lifespans, dead or euthanized-moribund cardiac modified *nmd* mice were subjected to a full necropsy examination; not only to establish the cause of death, but also to validate clinical diagnostic findings with grossly observed pathological changes. Although gross and microscopic alterations of the heart were observed, the cause of death was not exclusively cardiovascular in origin. Presumptively because of their underlying neuromuscular degeneration, *Cmn-nmd* mice like the transgenic rescued TgMI-*nmd* showed increased vulnerability to mega-esophagus and gastrointestinal motility disorders (data not shown). Hearts from *Cmn-nmd* mice with overt clinical signs revealed a range of morphological changes

including, but not exclusively, the presence of degenerating, apoptotic and necrotic, cardiomyocytes and replacement-interstitial fibrosis without inflammation. Furthermore, we did not observe pathognomonic pleural effusion previously associated with cardio-respiratory failure or secondary valvular insufficiency in *nmd* mice (5). In the extreme situation, however, signs of compensatory hypertrophic dilated cardiomyopathy were occasionally observed, suggesting a role for cardiac modifiers in promoting cardiovascular adaptation and remodeling in order to maintain tissue perfusion.

DISCUSSION

We have shown that muscle-specific expression of an *Ighmbp2* transgene in *nmd* mice prevents cardiomyocyte loss and restores normal cardiac morphology and function. This tissue-specific rescue of cardiomyopathy confirms the essential role of IGHMBP2 in the maintenance and survival of, not only neurons, but also cardiac and skeletal myocytes. Regardless of the severity and progression of the motor neuron disease, these transgenic TgMI-*nmd* mice failed to develop DCM that would have resulted in early lethality. Rather, their life-spans were markedly extended, albeit with severely restricted mobility, and were more prone to sibling competition and complications stemming from their underlying progressive paralysis. This experiment further suggests that the early lethality of *nmd* mice is primarily due to the development of DCM, not the progressive motor neuron disease (Fig. 2C–D). Autosomal recessive mutations in the human IGHMBP2 gene cause a phenotypically similar motor neuron disease, SMARD1 (4). Like the mutant *nmd* mouse, SMARD1 patients develop a progressive neurogenic muscular atrophy as infants. However, unlike SMARD1 patients, the absence of diaphragmatic paralysis and the prevalence of DCM in *nmd* mice suggest that these muscle tissues may be differentially spared and/or readily modified by background strain polymorphisms. Whether this is a species-specific manifestation or a consequence of residual *Ighmbp2* expression (20–25% of normal) from the hypomorphic *nmd* mutation (2) remains to be determined.

The Role of IGHMBP2 in Cardiac and Skeletal Muscles.

Gross morphological and histopathological examinations of mutant *nmd* hearts shortly after birth revealed no discernable abnormalities. However, this does not necessarily reflect the absence of pathology at the molecular or functional levels in these hearts. Indeed if this is the case, our original hypothesis that IGHMBP2 is not critical for normal cardiac morphogenesis may have to be revised. From birth until 7 days post-natal, the major cardiac myosin heavy chain (MHC) isoform in the mouse is beta-MHC (manifested by slower heart rates). Thereafter, complete transition to the adult alpha-MHC isoform (manifested by faster heart rates) occurs (19). Although this transition appears to occur normally in *nmd* mice based on extrapolation of functional and biochemical analysis in newly weaned 3-week-old mice, temporally regulated cardiac morphogenesis and functional markers will need to be examined in much younger (prenatal and newborn) *nmd* mice. Preliminary echocardiographic examination of newborn P0 *nmd* mice revealed a remarkable difference in heart rates in mutants compared to sib-controls. The mutant *nmd* mice showed almost 30% greater heart rates relative to sib-controls suggesting signs of precocious cardiac functional development. Thus, besides normal levels of IGHMBP2 being essential for cardiomyocyte maturation during this stage of rapid growth (3–6 weeks of age), it may also be critical for appropriate cardiomyocyte differentiation during early cardiac morphogenesis. The essential functions of IGHMBP2 in cardiac muscle, therefore, could be defined by proper temporal expression of muscle isoforms, adequate remodeling, and compensatory responses of the heart to changing load and demand. Given that IGHMBP2 is putatively involved in transcriptional activation or splicing, not only will altered expression of pro-survival and/or pro-apoptotic genes result in a cascade of signaling events culminating in apoptosis, but it may also promote changes in cellular development that could ultimately affect function (11,20,21). To date, descriptions of DCM in SMARD1 patients is lacking, however

five SMARD1 infants were described with cardiac arrhythmia (3,4,22,23) and treatments to prolong their lives may reveal a role for IGHMBP2 in human heart disease. Alternatively, the presence of background modifier genes that significantly alter the onset and duration of DCM in *nmd* mice suggests that similar genetic modifiers may exist in humans to suppress or enhance the manifestation of DCM in SMARD1 patients.

Cardiac-Specific Genetic Modifiers Prolong the Lifespan of nmd Mice.

Although the cardiac modified Cmn^{C}-*nmd* mice display a remarkable amelioration of DCM, they still succumb to CHF and premature death. In contrast, the transgenic TgMI-*nmd* mice show complete cardiac rescue, suggesting that the protective alleles of the cardiac modifier loci can only partially suppress the cardiomyocyte degeneration. At the N4 and N5 backcross generations of B6.CAST-$Cmn^{C};Mnm^{C};Ighmbp2^{nmd\text{-}2J}$ mice, the mean lifespan and cumulative survival of these mice is significantly greater than *nmd* mice without the CAST-derived cardiac-specific modifier loci (Figure 5). Effective treatments for cardiomyopathic diseases such as Familial, Idiopathic and/or Hypertrophic Dilated Cardiomyopathy beyond heart transplant are currently not available (24). Our previous transgenic rescue of the neuromuscular degeneration phenotype (5) and now the cardiomyocyte degeneration in *nmd* mice offer the promise for an effective gene therapy. Apparent functional rescue of the *nmd* phenotype was achieved by transgenic expression of IGHMBP2 in motor neurons and in cardiac and skeletal myocytes. Moreover, the identification of genetic modifier loci delaying the onset and progression of cardiomyopathy in *nmd* mice suggest that molecular pathways exist that can be targeted to alter the pathogenesis of congestive heart failure.

MATERIALS AND METHODS

Generation and Characterization of Transgenic nmd Mice

Mice were bred and maintained under standard conditions in the Research Animal Facility at The Jackson Laboratory with Institutional Animal Care and Use Committee approval. For construction of the *Ttn-Ighmbp2* transgene, a 5.87 kb mouse genomic fragment corresponding to 76,880,200-76,874,334 bp (Chromosome 2 NCBI build-m33) was amplified from a 129-strain BAC CITB-305G19 encompassing the *Ttn* 5' region (25) using primers TTN64F (5'-CTGTCATTCAATCTTCCTGACAGTACTTTG-3') and TTN63R (5'-GGTGCTTGAGTAGTACTCTTTTCAGGCAC-3'). A T-A substitution (underlined-TTN64F) creates a Sca1 restriction site, and a CA-AC substitution (underlined-TTN63R) alters the *Ttn* start codon (ATG to AGT). This fragment was subcloned and sequenced in pCR4-TOPO (Invitrogen) and transferred to the pBSXtra-Ighmbp2 cDNA and SV40 poly(A) vector by EcoR1 digestion as described (5). T wo transgenic founders (45 and 108) of C57BL/6J-Tg (*Ttn-Ighmbp2*)/Cx mice were identified from tail genomic DNA using TTN88F (5'-CAACTGCATAAGCACCAGGAG-3') and Ighmbp2R17 (5'-GAGGTGAAGCTGTTGCTAGG-3') generating a 565 bp PCR product. B6-TgMI was bred to B6.BKS-$Ighmbp2^{nmd\text{-}2J}$/+ mice. Transgenic-+/*nmd* F1 offspring were further backcrossed to generate transgenic *nmd*/*nmd* (TgMI-*nmd*) mice. The $Ighmbp2^{nmd\text{-}2J}$ mutation was genotyped as described (5). All *nmd* mice and age-matched controls were weighed weekly prior to the onset of clinical signs up to 22-weeks.

Plasma Creatine Kinase (CK)

Blood was obtained from the peri-orbital sinus using heparinized microhematocrit tubes after application of Tetracaine topical anesthetic; plasma total CK and cardiac-derived CK-MB levels were assayed as described (5).

Cardiac Function and Histopathology

Measurements of systolic blood pressure and pulse rate were performed as described (5). Standard ECG and echocardiogram was performed in anesthetized mice (1–1.5% isofluorane in O_2 at 0.6 L/min) as described (5). Following ECG recording, hearts were isolated and fixed for at least 24 hours, processed and stained for histopathology as described (5).

Quantitative Trait Locus Analysis

Two backcross generations (N2) with an established parental congenic, B6.CAST-*Mnm*^{C} *Ighmbp2*$^{nmd\text{-}2J}$/+ as recipient and CAST/EiJ as parental donor strain were created. Of 850 total progeny, ~20% (166) were homozygous *nmd/nmd* and were aged until development of DCM. The CAST-derived *Mnm*^{C} modifier (Chr. 13) was fixed in the cross to avoid confounding effects of paralysis on maximum lifespan. Genotype analyses for *Mnm*^{C} and *nmd* loci were performed as described(5). Tail DNA from 166 *nmd/nmd* N2 progeny were PCR-amplified with SSLP markers (Invitrogen) as described (5). A total of 134 markers spaced at 10-20 cM, polymorphic between B6 and CAST, were typed on each of the 19 autosomes. Genotype-to-maximum lifespan correlations were performed using 40 short-lived and 40 long-lived male and female N2 *nmd/nmd* mice using Map Manager. Independent confirmation was carried out on all 82 *nmd* males and 84 *nmd* females using the PSEUDOMARKER set of QTL programs developed by Sen and Churchill (26). For further details and information: http://www.jax.org/staff/churchill/labsite/. Pairwise genome scans were conducted to search for interacting QTL pairs correlated with short or prolonged life-spans. A separate genome scan analysis was performed using sex as both an additive and interacting covariate.

RT-PCR Analysis

Total heart RNA was prepared from newborn (P0), P21, and P28 *nmd/nmd* and age-matched littermates using the Trizol method (Invitrogen) according to the manufacturer's instructions. For RT-PCR, 1 μg of total RNA from *nmd* mutant and control tissues were reversed transcribed using random hexamers and oligo dT as described (2). Primers within exon 1 of the *Ttn* gene (TTN50F 5'-TTCATGTCGGAGATGGTTGG-3') and within the *Ighmbp2* cDNA (*Ighmbp2*-R17) were used to generate a 600 bp transgene-specific RT–PCR product.

Statistical Analysis

Values were expressed as the mean ± SE and analyzed by paired Student's t-test or ANOVA using Statview 5.0.1 (SAS Institute Inc). A value of $P \leq 0.05$ was considered statistically significant.

Acknowledgements

We are grateful to Drs. Jane Barker, Beverly Paigen, and Mary Ann Handel for critical review of the manuscript. This work was supported by a grant from NIH RO1AR49043 to G.A.C.; T.P.M. was supported by fellowships from NIH T32 RR07068 and The American Heart Association. Scientific services at TJL supported in part by NCI-CA34196 (NIH Cancer Center Grant).

References

1. Morita H, Seidman J, Seidman CE. Genetic causes of human heart failure. J Clin Invest 2005;115:518–526. [PubMed: 15765133]
2. Cox GA, Mahaffey CL, Frankel WN. Identification of the mouse neuromuscular degeneration gene and mapping of a second site suppressor allele. Neuron 1998;21:1327–1337. [PubMed: 9883726]
3. Pitt M, Houlden H, Jacobs J, Mok Q, Harding B, Reilly M, Surtees R. Severe infantile neuropathy with diaphragmatic weakness and its relationship to SMARD1. Brain 2003;126:2682–2692. [PubMed: 14506069]

4. Grohmann K, Schuelke M, Diers A, Hoffmann K, Lucke B, Adams C, Bertini E, Leonhardt-Horti H, Muntoni F, Ouvrier R, et al. Mutations in the gene encoding immunoglobulin mu-binding protein 2 cause spinal muscular atrophy with respiratory distress type 1. Nat Genet 2001;29:75–77. [PubMed: 11528396]

5. Maddatu TP, Garvey SM, Schroeder DG, Hampton TG, Cox GA. Transgenic rescue of neurogenic atrophy in the nmd mouse reveals a role for Ighmbp2 in dilated cardiomyopathy. Hum Mol Genet 2004;13:1105–1115. [PubMed: 15069027]

6. Ross J Jr. Dilated cardiomyopathy: concepts derived from gene deficient and transgenic animal models. Circ J 2002;66:219–224. [PubMed: 11922267]

7. Pyle WG, Solaro RJ. At the crossroads of myocardial signaling: the role of Z-discs in intracellular signaling and cardiac function. Circ Res 2004;94:296–305. [PubMed: 14976140]

8. Nicol RL, Frey N, Olson EN. From the sarcomere to the nucleus: role of genetics and signaling in structural heart disease. Annu Rev Genomics Hum Genet 2000;1:179–223. [PubMed: 11701629]

9. Wallace DC. Mitochondrial defects in cardiomyopathy and neuromuscular disease. Am Heart J 2000;139:S70–85. [PubMed: 10650320]

10. Czubryt MP, Olson EN. Balancing contractility and energy production: the role of myocyte enhancer factor 2 (MEF2) in cardiac hypertrophy. Recent Prog Horm Res 2004;59:105–124. [PubMed: 14749499]

11. Wencker D, Chandra M, Nguyen K, Miao W, Garantziotis S, Factor SM, Shirani J, Armstrong RC, Kitsis RN. A mechanistic role for cardiac myocyte apoptosis in heart failure. J Clin Invest 2003;111:1497–1504. [PubMed: 12750399]

12. Crone SA, Zhao YY, Fan L, Gu Y, Minamisawa S, Liu Y, Peterson KL, Chen J, Kahn R, Condorelli G, et al. ErbB2 is essential in the prevention of dilated cardiomyopathy. Nat Med 2002;8:459–465. [PubMed: 11984589]

13. Erickson SL, O'Shea KS, Ghaboosi N, Loverro L, Frantz G, Bauer M, Lu LH, Moore MW. ErbB3 is required for normal cerebellar and cardiac development: a comparison with ErbB2-and heregulin-deficient mice. Development 1997;124:4999–5011. [PubMed: 9362461]

14. Grohmann K, Rossoll W, Kobsar I, Holtmann B, Jablonka S, Wessig C, Stoltenburg-Didinger G, Fischer U, Hubner C, Martini R, et al. Characterization of Ighmbp2 in motor neurons and implications for the pathomechanism in a mouse model of human spinal muscular atrophy with respiratory distress type 1 (SMARD1). Hum Mol Genet 2004;13:2031–2042. [PubMed: 15269181]

15. Pasotti M, Repetto A, Tavazzi L, Arbustini E. Genetic predisposition to heart failure. Med Clin North Am 2004;88:1173–1192. [PubMed: 15331312]

16. Darvasi A. Experimental strategies for the genetic dissection of complex traits in animal models. Nat Genet 1998;18:19–24. [PubMed: 9425894]

17. Suzuki M, Carlson KM, Marchuk DA, Rockman HA. Genetic modifier loci affecting survival and cardiac function in murine dilated cardiomyopathy. Circulation 2002;105:1824–1829. [PubMed: 11956126]

18. Le Corvoisier P, Park HY, Carlson KM, Marchuk DA, Rockman HA. Multiple quantitative trait loci modify the heart failure phenotype in murine cardiomyopathy. Hum Mol Genet 2003;12:3097–3107. [PubMed: 14519689]

19. Fijnvandraat AC, Lekanne Deprez RH, Moorman AF. Development of heart muscle-cell diversity: a help or a hindrance for phenotyping embryonic stem cell- derived cardiomyocytes. Cardiovasc Res 2003;58:303–312. [PubMed: 12757865]

20. Sabbah HN, Sharov VG. Apoptosis in heart failure. Prog Cardiovasc Dis 1998;40:549–562. [PubMed: 9647609]

21. Russo GL, Russo M. Ins and outs of apoptosis in cardiovascular diseases. Nutr Metab Cardiovasc Dis 2003;13:291–300. [PubMed: 14717062]

22. Grohmann K, Varon R, Stolz P, Schuelke M, Janetzki C, Bertini E, Bushby K, Muntoni F, Ouvrier R, Van Maldergem L, et al. Infantile spinal muscular atrophy with respiratory distress type 1 (SMARD1). Ann Neurol 2003;54:719–724. [PubMed: 14681881]

23. Rudnik-Schoneborn S, Stolz P, Varon R, Grohmann K, Schachtele M, Ketelsen UP, Stavrou D, Kurz H, Hubner C, Zerres K. Long-term observations of patients with infantile spinal muscular atrophy

with respiratory distress type 1 (SMARD1). Neuropediatrics 2004;35:174–182. [PubMed: 15248100]

24. Jain P, Massie BM, Gattis WA, Klein L, Gheorghiade M. Current medical treatment for the exacerbation of chronic heart failure resulting in hospitalization. Am Heart J 2003;145:S3–17. [PubMed: 12594447]
25. Garvey SM, Rajan C, Lerner AP, Frankel WN, Cox GA. The muscular dystrophy with myositis (mdm) mouse mutation disrupts a skeletal muscle-specific domain of titin. Genomics 2002;79:146–149. [PubMed: 11829483]
26. Sen S, Churchill GA. A statistical framework for quantitative trait mapping. Genetics 2001;159:371–387. [PubMed: 11560912]

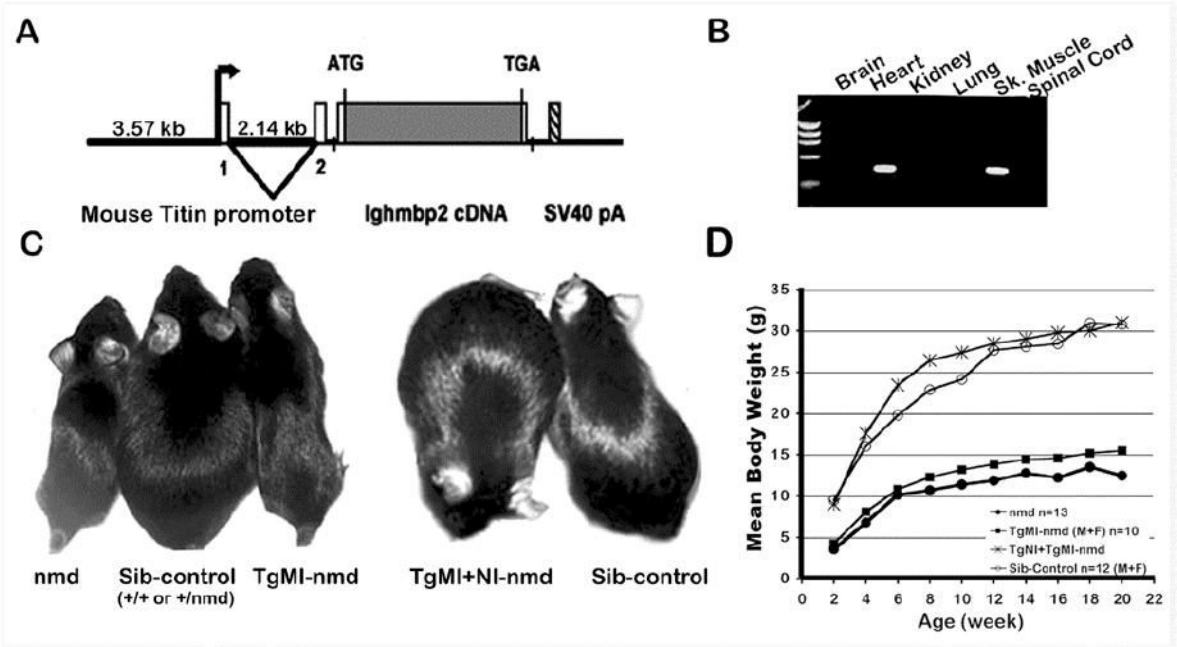

Figure 1.

(**A**) TgMI transgenic construct with the mouse titin promoter (containing 3.57 kb of upstream sequences, the complete noncoding exon 1 and intron 1, and 30 bp partial exon 2 sequence with mutated *Ttn* ATG to AGT) upstream of a wild-type mouse *Ighmbp2* cDNA and an SV40 polyadenylation signal. (**B**) RT-PCR assay for transgene expression in multiple tissues using transgene-specific primers (exon 1 of *Ttn* promoter and *Ighmbp2* cDNA reverse primer). (**C**) Live-photograph of a (L to R) B6-*nmd* mouse along with an unaffected and transgenic TgMI-*nmd* littermate at 6 weeks of age. Note that the TgMI transgene does not rescue the *nmd* paralysis phenotype, as the TgMI-*Ighmbp2* cDNA is not expressed in spinal cord (see **1B**). In contrast, 6-month-old double transgenic TgMI+TgNI-*nmd* mouse shows complete rescue of both the cardiomyopathy and neurogenic atrophy pictured next to its littermate. (**D**) Growth curve for the groups of mice in panel **C**.

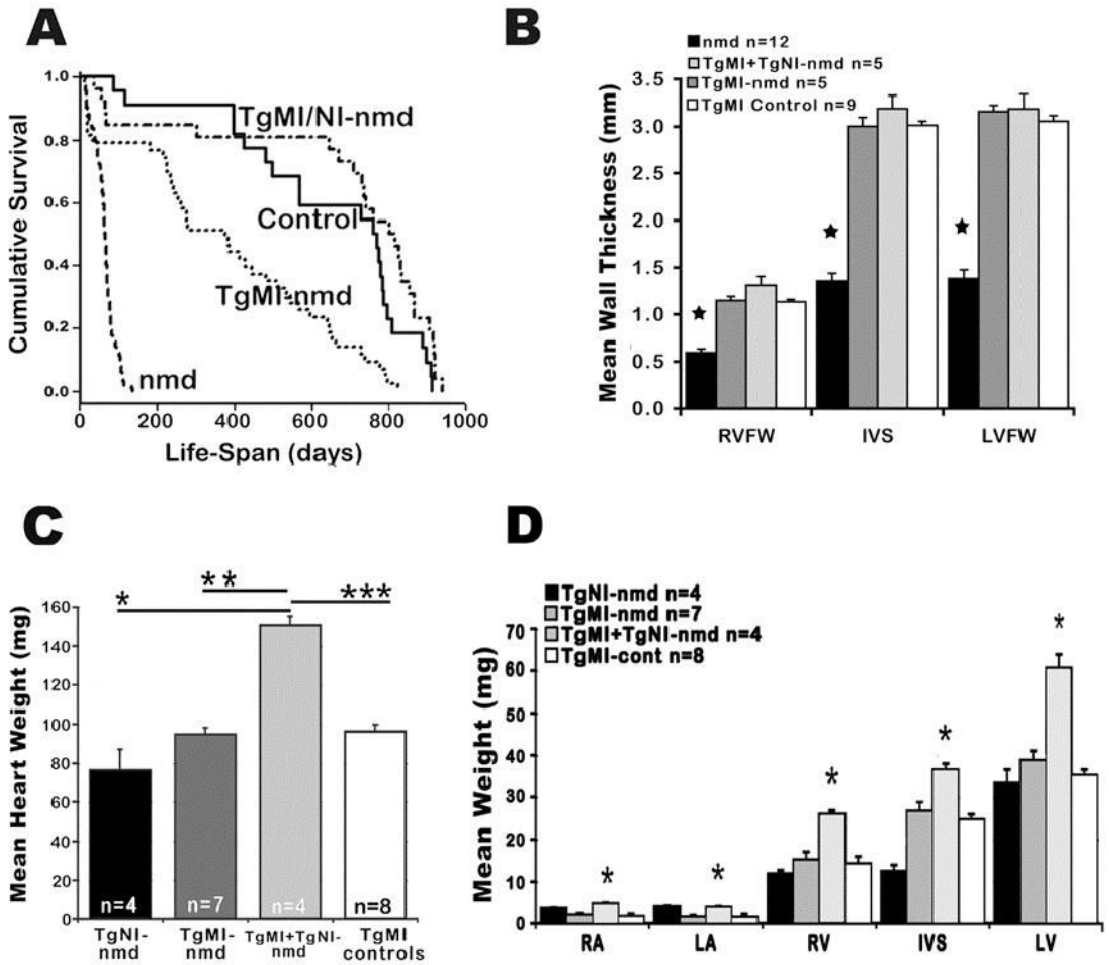

Figure 2.

(**A**) Cumulative survival curve for *nmd* (n=135), TgMI-*nmd* (n=43), double transgenic TgMI +TgNI-*nmd* (n=26) and sib-controls (n=22). (**B)** Histo-morphometric evaluation of ventricular wall thickness. (RVFW = right ventricular free wall, IVS = interventricular septum, LVFW = left ventricular free wall) (**C**) Mean heart weights of adult transgenic and non-transgenic *nmd* mice at 3 to 8-month of age and their age-matched transgenic (*+/+ or +/nmd)* sib-controls. (**D**) Mean wet-weights of individual cardiac chambers walls (RA = right atrium, LA = left atrium, RV = right ventricle, IVS = interventricular septum, LV = left ventricle).

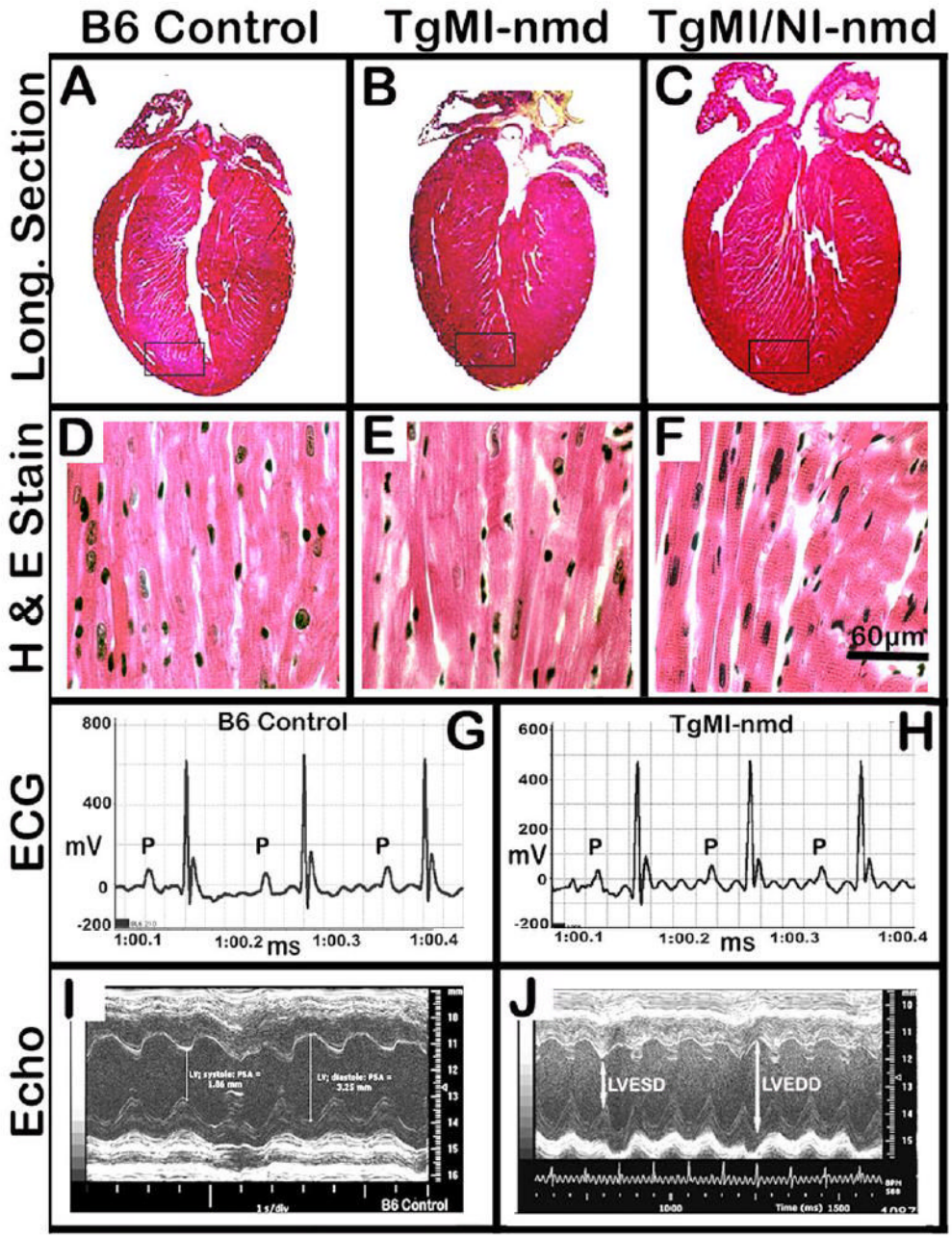

Figure 3.

Gross morphology, histology, electrocardiographic, and echocardiographic presentations of B6-control versus TgMI transgenic rescued *nmd* hearts at 8–16 week-of age. H & E-stained longitudinal sections in panels **A–C** show normal morphologic appearance of the heart. Magnification of the rectangular areas near the cardiac apex show cardiomyocytes staining uniformly- indicating a lack of pathological changes in panels **E** and **F** similar to B6-control in panel **D**. These observations are consistent with a normal ECG pattern in panel **H** analogous to a B6-control in panel **G,** both indicative of healthy cardiac conduction. Normal echocardiograms, manifested by relatively robust LVEDD and LVESD in panel **J** similar to B6-control in panel **I,** further attest to the cardiac rescue.

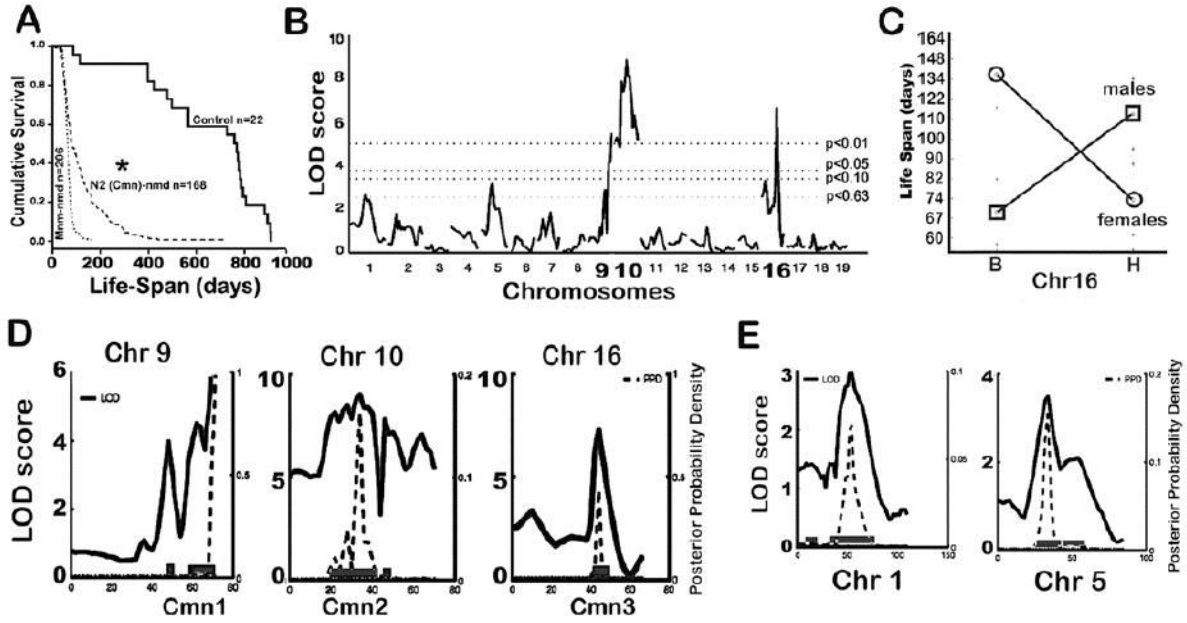

Figure 4

. (**A**) Cumulative survival rates of B6.CAST-*Mnm*^{C}-*nmd* mice with the neuron-specific modifier compared with the *N2 backcross *nmd* population used for QTL analysis and unaffected (*+/+ or +/nmd*) sib-controls. (**B**) Genome-wide screen of N2 backcross *nmd* mice and QTL analysis of maximum lifespan revealed significant linkage of CAST-derived modifier loci to Chromosomes 9, 10, and 16. The horizontal lines from bottom-up represent significance thresholds 0.63, 0.10, 0.05 and 0.01, respectively. (**C**) Gender-effect of the Chr. 16 CAST-modifier in males is significantly associated with increased lifespan, in contrast to females with a B6 allele beneficial to survival. (**D**) Interval map of each lifespan QTL with logarithm of odds (LOD) scores (solid line) and 95% confidence intervals. (**E**) Interval map of two suggestive B6-derived QTLs on Chrs 1 and 5.

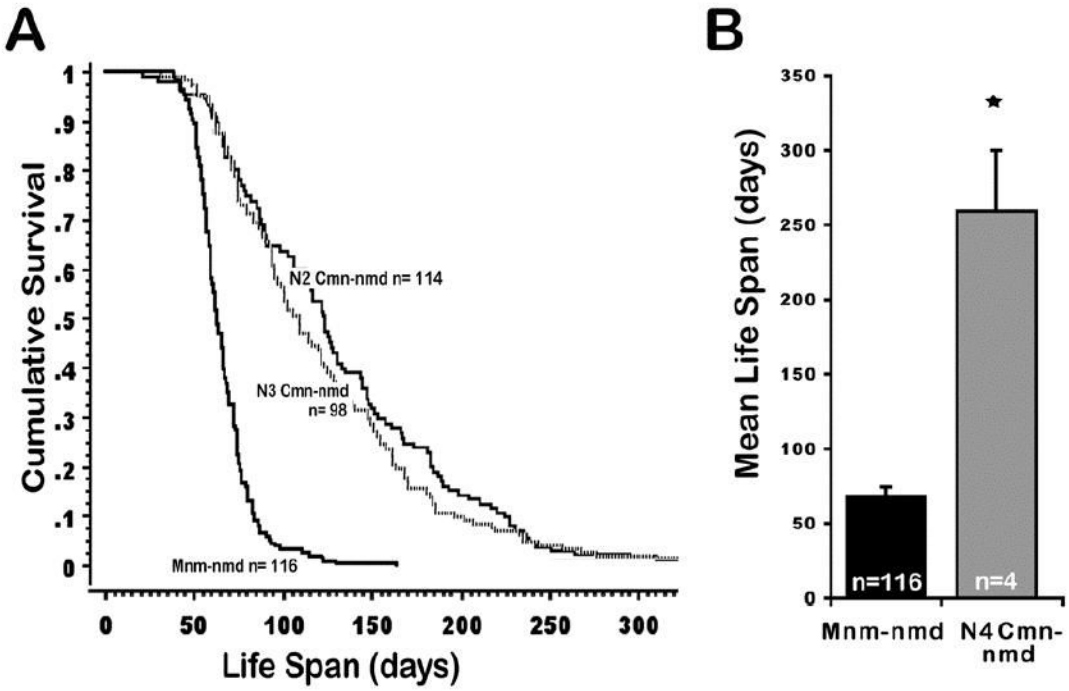

Figure 5.

(A) Cumulative survival curves of B6-*Mnm*^{C} *nmd* mice without CAST-derived cardiac modifiers and *Cmn-nmd* mice segregating modifier QTLs at the N2-N3 generations. **(B)** Mutant *nmd* mice heterozygous for *Cmn1, Cmn2, and Cmn3* loci at the N4 backcross generation lived significantly longer than B6-*Mnm*^{C}*-nmd* mice (*p < 0.0001).

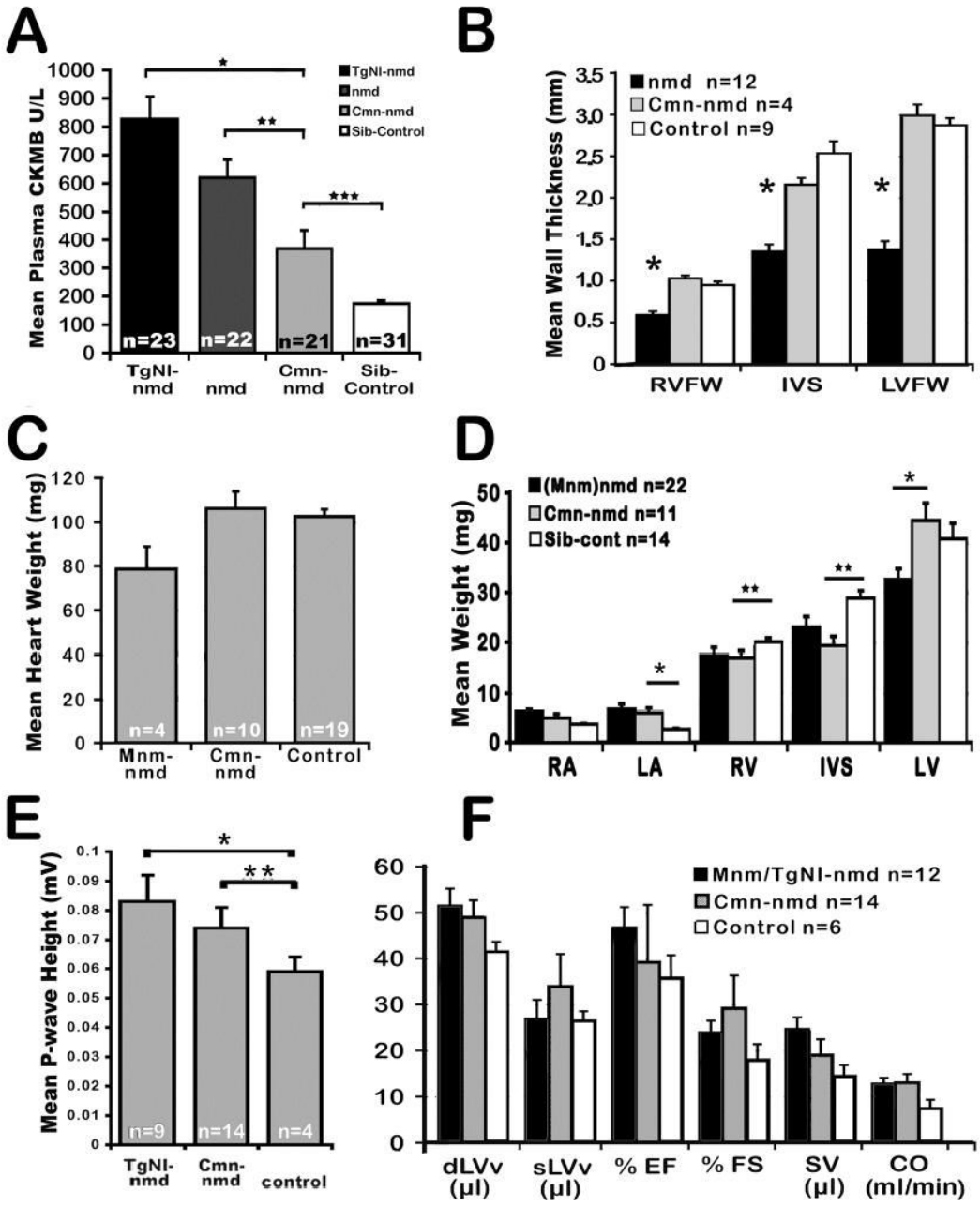

Figure 6

. (**A**) Plasma CKMB levels of 4-8 week old TgNI-*nmd* or B6-*nmd* and adult (6–8 month) N4F1 *Cmn-nmd* and age-matched littermates. (**B**) Mean ventricular free-wall thickness of 5–8 week old *nmd*, N3-N5 generation *Cmn-nmd* and unaffected littermates. (**C**) No significant differences are observed in the total heart wet-weights of B6.CAST-*Mnm-nmd*, N3-N6 *Cmn-nmd* or controls. However, wet-weights of individual cardiac chamber walls (**D**) do reveal significant differences. (**E)** Significant elevations of mean P-wave ECG amplitudes are evident in mutant *nmd* hearts carrying either the neuron-specific TgNI-transgene or *Cmn* cardiac modifiers compared to unaffected littermates, *p = 0.002 and **p = 0.009. (**F**) Derived cardiac functional parameters in B6-*nmd* mice and N3F1-N4F1 generation carriers of cardiac modifiers

versus sib-controls (dLVv = left ventricular volume at diastole; sLVv = left ventricular volume at systole; EF = ejection fraction; FS = fractional shortening; SV = stroke volume; CO = cardiac output).

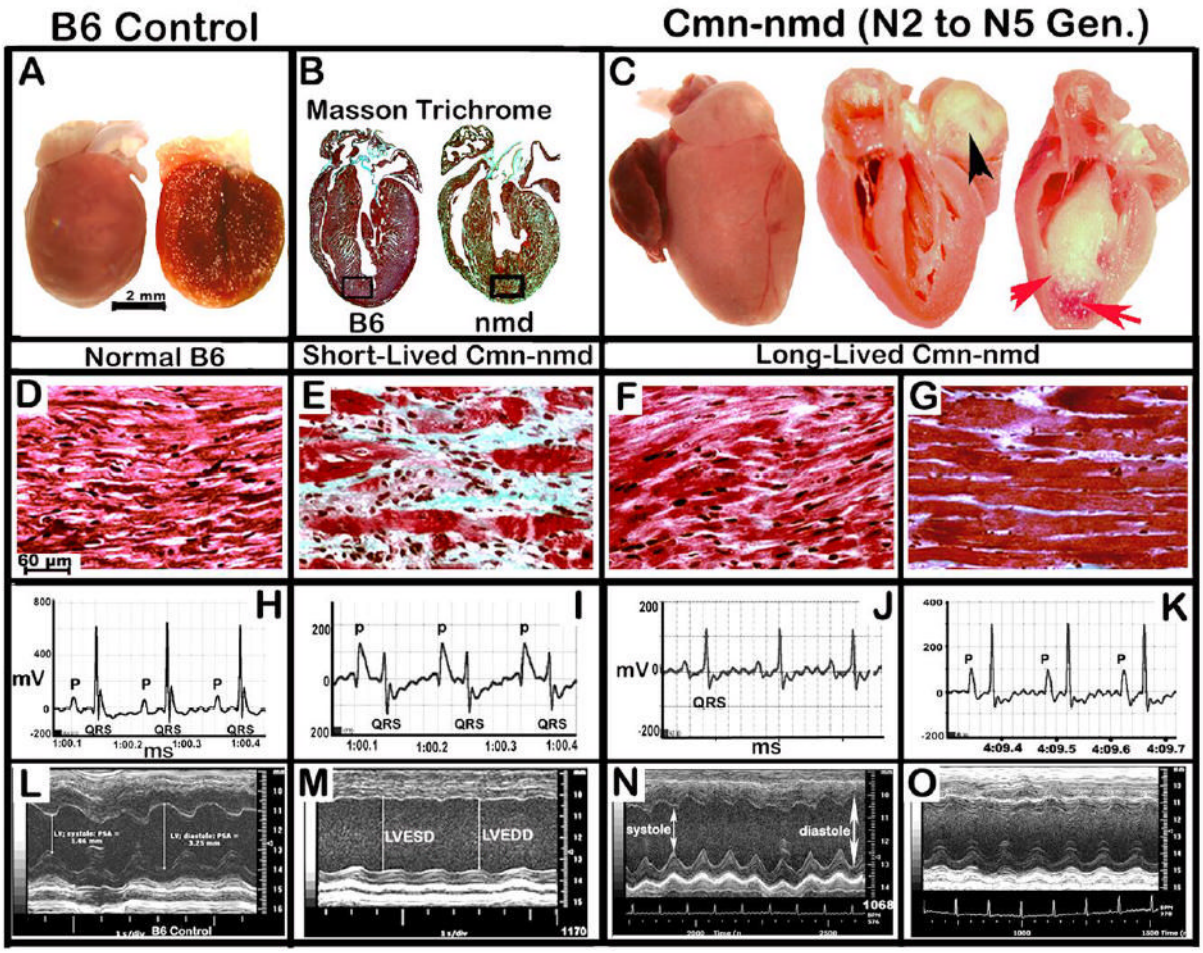

Figure 7.

(A and C) Gross morphologic presentation of B6-control and cardiac modified B6.CAST-*Cmn, nmd* hearts. **(B)** Masson Trichrome stained longitudinal sections of B6 and *Cmn-nmd* hearts. Rectangular areas near the apex of the hearts were magnified to show details as depicted in panels **D–G**. Unlike the short-lived *Cmn-nmd* heart in panel **E**, hearts from long-lived *Cmn-nmd* mice in **F** and **G** show dramatically less fibrosis. Cardiac function was evaluated using both ECG (**H–K**) and ultrasound examinations (**L–O**). Consistent with the p-wave enlargement and shortened QRS-complex in **I,** the presence of atrial enlargement, fibrosis, and markedly dilated ventricles on gross examination (**B and C**) is the appearance of functionally deficient cardiac contraction in panel **M**; depicted by LVEDD and LVESD.

Table 1

Chromosomal location and LOD scores for *nmd* lifespan QTLs

Name	Chr	Peak cM	95% CI cM	High Allele	Peak Marker	LOD	% Variance
Cmn1	9	70	60–70	CAST	*D9Mit17*	5.56	8.2
Cmn2	10	34	28–44	CAST	*D10Mit42*	7.95	12.1
Cmn3	16	44	42–48	CAST	*D16Mit64*	4.28	6.2

Cmn, cardiac modifier of *nmd*; Chr, chromosome; CI, confidence interval; LOD, logarithm of the odds ratio.